Recent progress in extending the cycle-life of secondary Zn-air batteries

Bagas Prakoso,[a] Muhammad Adib Abdillah Mahbub,[a] Meltem Yilmaz,[b,c] Khoiruddin,[d] I Gede Wenten,[d] Albertus Denny Handoko,*[c] Afriyanti Sumboja*[a]

[a] B. Prakoso, M. A. A. Mahbub, Dr. A. Sumboja
Material Science and Engineering Research Group, Faculty of Mechanical and Aerospace Engineering
Institut Teknologi Bandung
Jl. Ganesha 10, Bandung, 40132, Indonesia
E-mail: afriyanti.sumboja@material.itb.ac.id
[b] M. Yilmaz
Department of Chemistry
University College London
20 Gordon St., London WC1H0AJ, UK
[c] M. Yilmaz, Dr. A. D. Handoko
Institute of Materials Research and Engineering
Agency for Science, Technology and Research (A*STAR)
2 Fusionopolis Way, Innovis, Singapore 138634, Singapore
E-mail: adhandoko@imre.a-star.edu.sg
[d] Khoiruddin, Prof. I. G. Wenten
Department of Chemical Engineering
Institut Teknologi Bandung
Jl. Ganesha 10, Bandung, 40132, Indonesia

Abstract: Secondary Zn-air batteries with stable voltage and long cycle-life are of immediate interest to meet global energy storage needs at various scales. Although primary Zn-air batteries have been widely used since the early 1930s, large-scale development of electrically rechargeable variants has not been realized due to their short cycle-life. In this work, we review some of the most recent and effective strategies to extend the cycle-life of Zn-air batteries. Firstly, diverse degradation routes in Zn-air batteries will be discussed, linking commonly observed failure modes with the possible mechanisms and root causes. Next, we evaluate the most recent and effective strategies aimed at tackling individual or multiple of these degradation routes. Both aspects of cell architecture design and materials engineering of the electrodes and the electrolytes will be thoroughly covered. Finally, we offer our perspective on how the cycle-life of Zn-air batteries can be extended with concerted and tailored research directions to pave the way for their use as the most promising secondary battery system of the future

1. Introductions

Rapidly changing climate and ballooning energy demands due to rapid population explosion and intense industrialization have urged societies to shift from fossil fuels to more sustainable energy sources.[10-12] Unfortunately, the transition towards renewable energy is uneven among different countries, limited by local conditions (e.g., political and societal landscape, geological area, economic condition, and industrial demand).[13] These challenges are exacerbated by the technical difficulties of integrating renewable technologies into existing power grids.[14-16] Advances in high capacity and efficient energy storage devices enable “smart grid” technology to improve energy distribution reliability and integrate renewable energy sources.[17, 18] Continuous development of high-performance energy storage devices, including batteries, is thus of utmost importance. Beyond grid-level energy storage, battery technologies with size and design flexibility while maintaining close to theoretical performance are indispensable for everyday life applications.[19]

Traditional secondary batteries (e.g., lead-acid, nickel-cadmium, or lithium-ion) have found their rooting in many portable electronic devices. Among them, lithium-ion batteries are arguably the most successful due to the high energy density, which can be deployed to larger-scale applications such as electric vehicles (EVs) and grid-scale energy storage solutions.[20-23] Despite these advantages, there are numerous safety and cost related concerns on lithium-ion batteries that have yet to be satisfactorily addressed. In particular, lithium’s extreme reactivity mandates inert production environment and the addition of additional protection circuitry to reduce the possibility of catastrophic failures. To this end, metal-air batteries can offer significant advantages over lithium-ion. Metal-air batteries exploit the abundant oxygen (O_2) in air as the active species, providing high energy density that is scalable, easily produced in large quantities, and inherently safe.[24-26] High energy densities can be attained for metal-air batteries as the active species (O_2) is not stored within the battery structure. Instead, it is taken from the atmosphere through the battery’s open architecture.[27, 28] However, to be applicable in large-scale and everyday life applications, key technical hurdles affecting the power density, electrolyte lifetime, and anode durability must first be addressed.

Various metals (e.g., Zn, Mg, Al, Fe, Li, Na, K) have been explored as the anode material in metal-air batteries. Li-air batteries are expected to deliver the highest energy density with theoretical specific energy of up to 13.5 kWh kg^{-1}.[29] However, the instability of lithium when directly exposed to O_2 or water poses serious safety issues.[30] Although not classified as a rare metal, the expansive demand for lithium is predicted to quickly outstrip the production rate,[31] leading to a possible scarcity and significant cost increase in the near future. Hence, more attention has been given to Zn-air batteries, a century-old technology that was first conceived in 1840.[32] Zn is particularly suitable for battery operation in an aqueous solution because it has a suitable redox potential of -0.76 V (vs. SHE) within the narrow operating window defined by the water-splitting process.[33] Zn-air batteries are a rising technology of choice in large-

scale energy storage due to their high energy density (1350 Wh kg^{-1}, theoretical), low production cost, good safety, and environmental friendliness.[34-36] They can be manufactured at a much lower cost than Li-ion batteries(<10$ $kW^{-1}h^{-1}$)[37] as zinc is much more abundant than lithium, with almost 200 times greater yearly global production capacity.[38] _ENREF_28 While primary Zn-air batteries have been widely used in hearing aids, navigation lights, railway signaling systems, and military applications,[39] the widespread use of secondary Zn-air batteries is yet to be realized due to the short (electrical) cycle-life. The lifetime issue is closely related to the multitude of undesirable changes in the anode, cathode, and electrolyte, which will be thoroughly reviewed in this work. New approaches and technologies that can counter some of these challenges will be discussed, complementing existing reviews on Zn-air batteries.[19, 40-45] We start with a brief overview of the rechargeable Zn-air battery, focusing on known contributing factors to the short cycle-life of Zn-air batteries and their possible root causes. Efforts to improve and extend the cycle-life of secondary Zn-air batteries will be discussed, not only from materials point of view, but also the cell designs. Together, perspectives on the future development of rechargeable Zn–air batteries will be discussed in the last part.

2. Working principles of Zn-air batteries

The construction of a typical Zn-air battery consists of a Zn anode, an air cathode, and an ion-conducting electrolyte (**Figure 1**). For many commercial Zn-air batteries, the anodes are usually composed of granulated zinc powders with some additives. The electrolyte serves as an ionic migration medium during the discharge/charge process. Therefore, the conductivity of the electrolyte is crucial in determining the overall electrical resistance of the battery. The cathode in Zn-air batteries, known as the “air cathode/electrode”, consists of a catalyst layer, a current collector, and gas diffusion layers (GDLs). The GDLs serve the dual purpose of conducting electricity and allowing the O_2 to enter the battery. Thus, it should possess low electrical resistance and desirable wetting characteristics for the particular electrolyte.[46] A separator may also be added in between the anode and the cathode to reduce cross-mixing of anolyte and catholyte, while still allowing facile ionic transportation to complete the electrochemical reaction circuit. Porous polymeric membranes are commonly used as separators, although they are not ideal as they cannot block cationic species produced during the anodic reaction, decreasing the capacity and lifetime of the battery. To improve this, certain types of membranes made of ionic exchange resin have been explored.[47]

The overall electricity storage and release in the Zn-air battery are facilitated by the redox reactions between the Zn anode and the air cathode (equation 2.1). During the discharge process, a partial oxygen reduction reaction (ORR) occurs at the air cathode, generating hydroxyl (OH^-) anionic species (equation 2.2). These OH^- ions then migrate closer to the Zn metal anode due to a concentration gradient, producing soluble zincate ions ($Zn(OH)_4^{2-}$, equation 2.3). In some conditions, the zincate ions dehydrate and precipitate as insoluble zinc oxide (ZnO, equation 2.4), which can block the active surface area when it is deposited onto the anode. Operation in a slightly acidic pH has been proposed to alleviate this issue.[48] A parasitic hydrogen evolution reaction (HER) can also take place (equation 2.5), generating reactive H_2 gas which can induce corrosion issues on the Zn anode. The generated electron then flows through the air electrodes, generating hydroxyl ions (OH^-) to further participate in the following redox reactions.

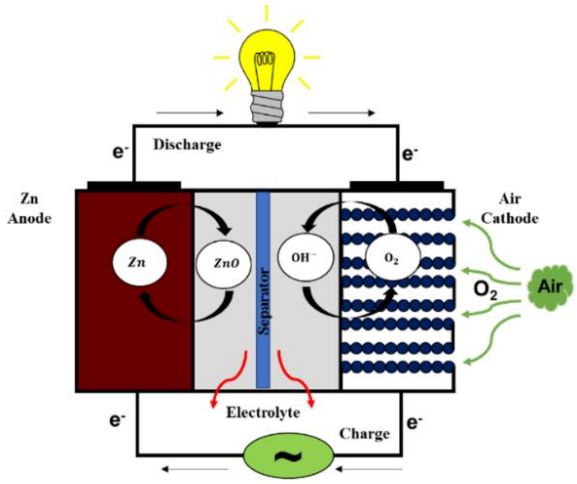

Overall : $2Zn + O_2 \leftrightarrow 2ZnO$ (2.1)

Air electrode : $\frac{1}{2}O_2 + 2e^- + H_2O \leftrightarrow 2OH^-$ (2.2)

Zn electrode : $Zn + 4OH^- \leftrightarrow Zn(OH)_4^{2-} + 2e^-$ (2.3)

$Zn(OH)_4^{2-} \leftrightarrow ZnO + 2OH^- + H_2O$ (2.4)

HER : $Zn + 2H_2O \leftrightarrow ZnO + H_2$ (2.5)

(OER ↔ ORR) : $O_2 + 4e^- + 2H_2O \leftrightarrow 4OH^-$ (2.6)

Figure 1. General configuration of a rechargeable Zn-air battery.

Alternatively, a complete four-electron ORR pathway may also occur at the air electrode (equation 2.6). For practical applications, this four electron pathway is highly desirable due to its high efficiency and the absence of detrimental peroxide species which could corrode the air cathode. This can be achieved by incorporating a bifunctional oxygen electrocatalyst within the air cathode.[49] The same catalyst will also be instrumental to the battery performance during the charging process, as the oxygen evolution reaction (OER) is operating (the reverse reaction of ORR).

3. Cycle-life degradation mechanism of Zn-air batteries

The cycle-life of a secondary battery is directly linked to its ability to maintain a stable charge-discharge performance before failure. The inferior cycle-life of electrically rechargeable Zn-air batteries has been a major block for their deployment in large-scale applications, especially in the grid energy storage and transportation sectors.[50, 51] The unsatisfactory cycling stability of Zn-air batteries can be associated with several phenomena at the anode, electrolyte, and air cathode. The degradation mechanism of each failure mode occurring at each component of Zn-air batteries and the expected failure outcomes are summarized in **Table 1**.

One key reasoning behind the instability and poor cycle-life of Zn-air batteries is the continuous structural changes taking place in the anode.[52-57] The structural changes can take the form of gross morphological changes, passivation, and dendrite formation on the Zn anode. Such changes are usually caused by non-uniform deposition/distribution of Zn element, leading to uneven anodic reaction and excessive formation of ZnO. In addition to the low cycling performance, shape changes and densification also reduce the effective surface area of Zn, resulting in lower discharge voltage and significant capacity loss due to poor utilization of the Zn anode. The formation of a passivating ZnO layer also hinders electron transfer and limits the hydroxyl or zincate ion mass transfer to/from the anode, further decreasing the batteries' performance. The excessive formation of dendrites may also damage the separator and reach the cathode side, causing the electrode shorting and catastrophic failure of the battery.[53, 54, 57] Moreover, the Zn anode may also experience a self-corrosion failure mode as a result of the HER at the anode. Rigorous HER processes may also consume part of the electrolyte and liberate significant amount of gas that can increase the internal pressure of the battery.[50, 52, 55, 56]

Changes in the electrolyte concentration will also affect the cycle-life of Zn-air batteries. The concentration change can be attributed to the water absorption (or evaporation) caused by the relative humidity differences with the ambient environment.[57, 58] A low ambient humidity encourages water evaporation from the electrolyte, causing the electrolyte to dry out. Electrolyte leakage and high-temperature operation bring similar effects, which reduces the performance and cycle-life of the Zn-air battery. Conversely, the high ambient humidity causes the accumulation of water droplets in the air cathode due to the alkaline electrode's quiescence. Besides humidity, atmospheric CO_2 may also react with the alkaline electrolyte due to the cell's open infrastructure, forming soluble and insoluble carbonates. The soluble carbonate formation will gradually reduce the electrolyte conductivity due to its low dissociation constant. The precipitation of insoluble carbonates will reduce the cation concentration, consume the electrolytes, and create undesirable deposits. In addition, these deposits may block the pores of the air cathode, which will gradually degrade the cycle-life of the battery.[59]

The structural changes in the air cathode may happen either at the catalyst layer or at the GDLs. Both layers may be corroded due to the use of high currents and concentrated alkaline electrolytes, which oxidize the catalyst layer and/or GDLs. During a prolonged cycle, the catalyst particles may be lost due to their poor attachment to the GDLs and the formation of oxygen bubbles during charging may occur as the product of the OER. The formation of oxygen bubbles may prevent the electrolyte from reaching the catalyst layer, hindering the catalytic reaction and reducing the battery performance. The catalyst particles may also agglomerate, which reduces the catalytic activity and increase the resistance. Furthermore, carbonates clogging and electrolyte flooding in the air cathode must be prevented to ensure efficient triple-phase contact and reaction (electrolyte, catalyst, and oxygen).[51, 60]

4. Materials strategies to enhance the cycle-life of Zn-air batteries

4.1. Anode

To achieve excellent capacity retention, a multi-pronged strategy needs to be pursued in all its components. On the anode side, altering the materials composition is a common strategy, as introducing a foreign element such as alloying components or in minute concentration as impurities can affect the electrochemical behavior significantly.[61] Beyond composition alteration, various other approaches to improve the composition of the Zn anode have been explored, such as adding carbonaceous additives and introducing polymeric, organic, or inorganic coating. The most recent approaches, categorised based on the battery component, are summarized in **Table 2**. Many of these strategies aim to facilitate the direct dissolution of Zn ions without the formation of intermediate species, suppressing water splitting (forming either H_2 or O_2) and discouraging dendrite formation. We will elaborate on the most effective strategies in this section.

Lysgaard et al.(2018) showed that alloying Zn with heavy metals, such as bismuth and indium, improved the stability of the Zn-air battery.[62] It was proposed that the incorporation of bismuth stabilized the battery's discharge potential, whereas indium could suppress the HER during battery operation. Lee et al.(2019) demonstrated that a composite of copper oxide and zinc (CuO-Zn) was able to reduce the corrosion and dendrite formation.[7] Incorporation of 0.5 wt% CuO in the Zn anode resulted in a higher hydrogen overpotential, which decreased the corrosion due to HER in the Zn anode. Furthermore, the addition of CuO resulted in more uniform zinc deposits on the anode (**Figure 2a**). The reduced CuO served as deposition spots for Zn^{2+} that helped produce uniform zinc deposits and control the dendrite formation. Zn anode with the addition of 0.5 wt% CuO was able to maintain stable performance for 19 cycles (19 hours testing time) during the charge-discharge measurement.

Organic additives, such as polymeric binders, have been added together with the conductive agents to minimize the shape change and restrain the passivation growth on the Zn anode, resulting in a better cycle-life in the Zn-air battery.[63] Carbon-based materials such as carbon black and graphene/graphene oxide (GO) have been used as conductive agents in the anode.[64-66] Lee et al.(2017) reported that using Super-P carbon as a conductive additive could enhance the rechargeability by providing reliable electronic paths among the Zn particles.[67] Other work by Zhou et al.(2019) demonstrated that GO-modified Zn anode was able to prevent the

passivation and dissolution problems.[68] The incorporation of GO resulted in improved cycle-life for up to 200 cycles (~200 hours testing time) due to the well-distributed ZnO within the GO layers.

Table 1. Degradation mechanism of rechargeable Zn-air batteries

Degradation mode	Degradation mechanism	Failure outcome
Zn dendrite formation	Non-uniform Zn deposition on the anode surface	Short circuit
Zn anode shape change	Uneven reaction zone at the anode	Reduce anode active surface area
	Non-uniform Zn deposition at the anode surface	Reduced usable capacity & energy density
	Convective flow caused by the electro-osmotic force	
Zn anode passivation (densification)	Precipitation of insulating ZnO on the anode surface caused by the high concentration of zincate ($Zn(OH)_4^{2-}$) ion	Low conductivity of the anode Low practical voltage Poor rechargeability Loss of capacity and energy density
Corrosion at the carbon-based air cathode	High current density exposure during charging	Poor rechargeability of the battery Low cycle-life of the battery
Corrosion at the catalyst	Severe oxidation of the catalyst during oxygen evolution reaction	Poor rechargeability of the battery Low cycle-life of the battery
Loss of the catalyst	Poor configuration of the electrolyte flow Formation of oxygen bubbles during charging	Poor charging/discharging voltage of the battery Inferior ORR/OER performance
Agglomeration of the catalyst	High surface energy of the catalyst	High resistance at the catalyst/electrolyte interface Inferior ORR/OER performance Low cycle-life of the battery
Gas evolution (H_2)	The more negative potential of Zn reduction as compared to HER	Increase the internal pressure during charging Anode corrosion Reduce the active surface area Gradual loss of electrolyte
Gas evolution (O_2)	Reaction product during OER	Inhibited fluid motion within the gas diffusion layer Hinder the catalytic reactions at the air cathode Limit the capacity and energy density of the battery
Electrolyte concentration change	Electrolyte deliquescence in humid climate High operation temperature Electrolyte leakage Formation of discharge product	Water absorption increases internal resistance. Water evaporation → cell failure
Carbonate formation	Reaction product between alkaline electrolyte and ambient CO_2	Decrease the electrolyte conductivity Reduce the air cathode activity due to blocked electrocatalytic sites
Electrolyte leakage	Low hydrophobicity of the gas diffusion layer	Premature drying out of the cell Deterioration of the battery's capacity and cycle-life
Air cathode flooding	Penetration of electrolyte into air cathode caused by the low/loss of hydrophobicity of gas diffusion layer	Poor O_2 access to the catalyst layer Large overpotential during ORR

Coating with organic or other materials (e.g., polymer, metal oxide) also improves the Zn anode performance.[56, 69, 70] The coating layer reduces the problems associated with corrosion, dendrite formation, and shape change, by preventing excessive and undesirable reactions between Zn anode and electrolyte. Using this strategy, the hydroxyl ions can pass through the coating layer while $Zn(OH)_4^{2-}$ could effectively be blocked. Hence, dendrite growth and shape changes can be minimized, while maintaining battery performance. Xia et al.(2019) reported the use of self-assembled reduced graphene oxide (rGO), which served as a protective film to prevent the growth of Zn dendrite in the anode, resulting in excellent long term cycling performance of more than 1000 cycles (~1200 hours testing time).[71]

Recent work by Zhang et al.(2020) employed an interesting strategy of encasing submicron Zn anode with TiO_2.[8] It is proposed that the TiO_2 outer layer acts as an ion-sieving layer that blocks the larger zincate ions, while suppressing HER at the same time. Expectedly, the bare anode (ZnO rod) showed severe structural degradation after the charging process (**Figure 2b**). However, anodes coated with TiO_2 layer was able to maintain their original structure after five charge-discharge cycles. Using this coating strategy, the battery achieved a stable performance for 350 cycles (~700 hours testing time). In another recent study, Hao et al.(2020) succeeded in inhibiting the side reactions and dendrite growth by introducing artificial solid/electrolyte interphase (SEI) layer by using poly(vinyl butyral) (PVB).[9] The modified anode effectively blocked water from the Zn surface and maintained the uniform stripping/plating of Zn ions underneath the film. The Zn-air battery with this type of anode exhibited excellent cycling stability of 1500 cycles (~2200 hours testing time) at a current density of 0.5 mA cm^{-2} (**Figure 2c**).

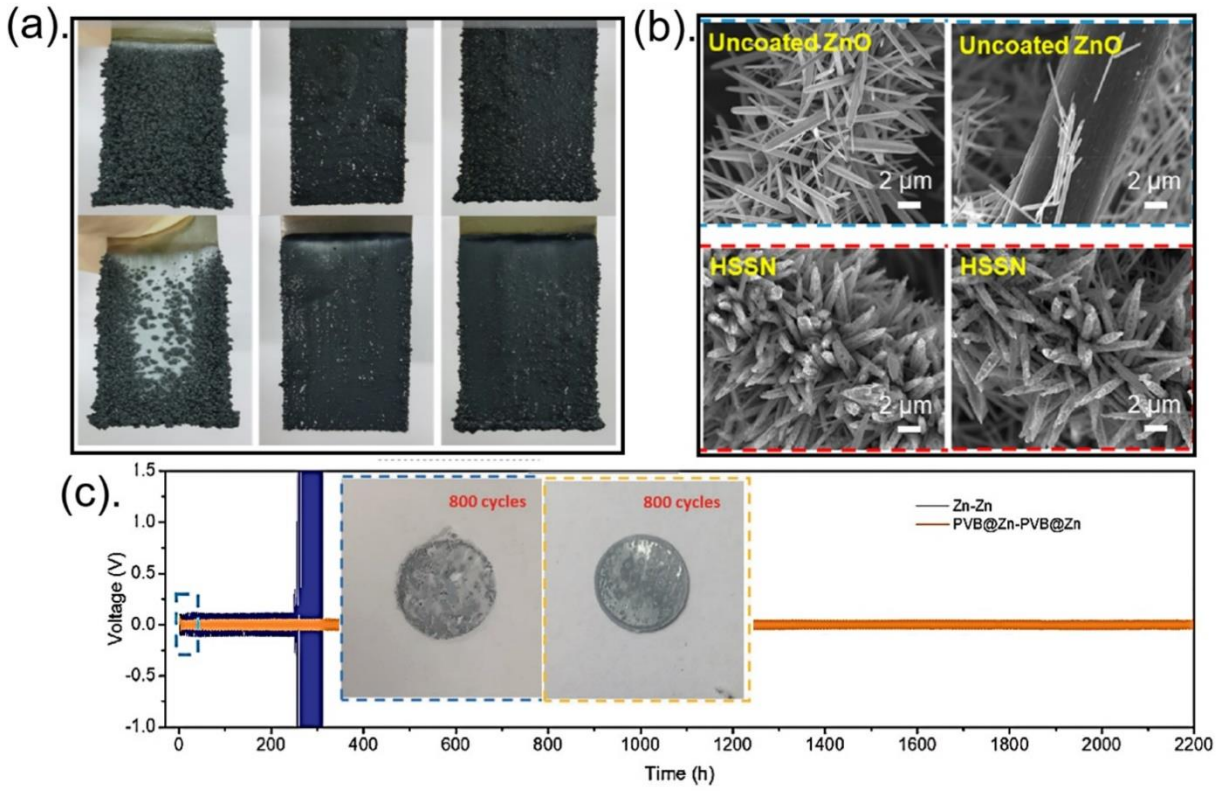

Figure 2. a) Photographs of Zn deposit without additives (left), with CuO (middle), and with $CuCl_2$ additives (right) on the front (top) and backside (bottom). b) SEM images of the uncoated ZnO anode and ZnO/TiO_2 (i.e., HSSN anode) before charging (left) and after charging (right). c) Cycling stability of Zn plating/stripping in both of bare Zn and poly(vinyl butyral) coated Zn (PVB@Zn) symmetric cells (Inset: Digital images of Zn electrodes (left) and PVB@Zn electrodes (right) that were stripped out of the cells after 800 cycles. (Adapted from ref. [7-9] with copyright permission from Elsevier, American Chemical Society, and John Wiley and Sons, respectively)

4.2. Cathode

Corrosion and flooding, as well as catalyst loss and agglomeration, are the most common problems associated with the air cathode which can decrease the cycle-life of Zn-air batteries.[72, 73] In this case, strategies to improve the stability of the air cathode can be done by improving the performance of the gas diffusion layer (GDL) and the bifunctional electrocatalysts. GDLs in Zn-air batteries are mostly based on carbon or nickel foams. While the raw material costs are relatively inexpensive, the actual cost of GDLs can be inflated due to the complex manufacturing process. Serious corrosion is commonly observed on both nickel and carbon-based GDLs, which precludes their application in long term rechargeable Zn-air batteries until suitable improvements are discovered. Furthermore, the pore structure of common carbon-based GDLs are typically unaligned, which has been shown deleterious to the oxygen permeability.[74] Hence, a slew of novel GDLs have been proposed recently to address the limitation of nickel and carbon-based GDLs.

A notable example is reported by Moni et al.(2020) where they synthesized silicon-based GDLs using the freeze tape casting technique.[74] The symmetric sponge-like structure of these silicon-based GDLs provided a shorter path for oxygen diffusion and electron transfer, allowing a higher O_2 exchange rate compared to carbon-based GDLs with unaligned pore structures. Secondary Zn-air batteries using these silicon-based GDLs showed a promising performance (~200 cycles/34 hours testing time), comparable to the battery with a commercial air cathode. In another report, Lee et al.(2019) developed an air cathode based on a fibrous mixture of NBSCFs ($NdBa_{0.5}Sr_{0.5}Co_{1.5}Fe_{0.5}O_{5+\delta}$ double perovskites), N-CNTs, and carbon nanofibers to obtain an air cathode that could effectively hinder the loss of catalysts due to its highly entangled network structure.[75] Zn-air battery with this air cathode maintained its charge and discharge voltage for up to 90 cycles (~15 hours testing time) without any apparent voltage fading.

Besides improving the quality of GDLs, effective and stable bifunctional electrocatalysts are also needed to improve the stability of Zn-air batteries. Comprehensive reviews on the development of bifunctional electrocatalysts for Zn-air batteries can be found in the literature.[42, 44, 76-78] A high-performance bifunctional electrocatalyst should possess a large number of active sites, desirable hydrophilic properties, superior conductivity, good chemical stability, and high corrosion/oxidation resistance. Besides that, good attachment of the catalysts onto the GDLs is desirable as it reduces the battery's resistance and prevents the detachment of the catalyst during the battery operation.

Table 2. Strategies to enhance cycling stability of secondary Zn-air batteries in literature

Strategy to enhance cycle-life	Anode	Catalyst/gas diffusion electrode*	Electrolyte	Current density (mA cm^{-2})†	Cycling stability (cycle/ hour)‡	Ref.
ANODE						
Additives at the anode	Zn/PAA/ KOH/C	-/C	6 M KOH	-	-	[67]
Additives at the anode	Zn/GO	-/NiOOH	4 M KOH/2 M KF/2 M K_2CO_3	1§	200 / 200	[68]
Alloyed anode	Zn/Ni/In	-/-	8.5 M KOH/ZnO/PEG	-	100 / -	[79]
Alloyed anode	Zn/In/Bi	-/$NiCo_2O_2$	6 M KOH	1	3 / 25	[62]
Coating the anode	Zn/Li_2O/ B_2O_3	-/C	KOH	164.1	-	[80]
Coating the anode	Zn/Al_2O_3	-/C	9 M KOH	10	20 / -	[56]
Coating the anode	Zn/RGO	-/C	0.5 M $ZnSO_4$	1	>1000 / 1200	[71]
Coating the anode	ZnO/TiO_2	-/-	4 M KOH	-	350 / 700	[8]
Coating the anode	Zn/PVB	MnO_2/C	1 M $ZnSO_4$/0.1 M $MnSO_4$	5‖	1500 / 2200	[9]
Composite anode	Zn/Al	-/$Ni(OH)_2$	6 M KOH/ZnO	1‖	1000 / -	[81]
Composite anode	Zn/CuO	-/-	4 M KOH/PAA	65¶	19 /19	[7]
AIR CATHODE						
Improving electrocatalyst	Zn	N,P-C/C	6 M KOH	2	180 / 30	[82]
Improving electrocatalyst	Zn	MnO_x/C	6 M KOH/ 20 gL^{-1} $ZnCl_2$	15	500 / 125	[83]
Improving electrocatalyst	Zn	MnO_x-Co/C	6 M KOH/0.15 M $ZnCl_2$	5	1200 / 200	[84]
Improving electrocatalyst	Zn	NiMn/C	6 M KOH/ 0.2 M ZnO	10	~259 / ~86	[85]
Improving electrocatalyst	Zn	MnO_x/C	CH_2=CHCOOH/ $C_7H_{10}N_2O_2$ /11.25 M KOH/0.25 M ZnO/0.33 M $K_2S_2O_4$	0.7	175 / ~66	[86]
Improving electrocatalyst	Zn	CoFe/N-C	6 M KOH/0.4 M $Zn(OAc)_2$	6.5	~500 / >140	[87]
Improving electrocatalyst	Zn	FeNi/N-C/C	18 M KOH/PVA	10	200 / ~33	[5]
Improving electrocatalyst	Zn	FeCo/FeCoNi/N-C	6 M KOH/0.2 M $Zn(OAc)_2$	5	1005 / 670	[6]
Improving electrocatalyst	Zn	FeNi/N-C	6 M KOH/0.2 M $ZnCl_2$	10	100 / -	[88]
Improving electrocatalyst	Zn	Ni/Ni-N-C/C	6 M KOH/0.2 M $C_4H_6O_4Zn{\cdot}2H_2O$	10	210 / 210	[89]
Improving electrocatalyst	Zn	$Ni_{1.5}Co_{1.5}S_4$/C	6.0 M KOH/0.1 M $Z(O_2CCH_3)_2$	4	~125 /~58	[90]
Improving electrocatalyst	Zn	MnO_x/C	6 M KOH/0.15 M ZnO	10	>200 /~70	[91]
Improving GDLs	Zn	Pt,Ru/C/SiOC	6 M KOH	3	204 / 34	[74]
Improving GDLs	Zn	C/PTFE/NBSCF/ N-C	6 M KOH/0.2 M $Zn(OAc)_2$	1	90 / 15	[75]
ELECTROLYTE						
Additives at the electrolyte	Zn/Nafion	-/-	4 M KOH/ ZnO/2 M KF/2 M K_2CO_3	1	10/300	[92]
Additives at the electrolyte	Zn	Co-Sn-C/Ni/Pd/SS	1 M KOH/0.1 g graphene	-	-	[93]
Ionic liquid electrolyte	Zn	-/$FeFe(CN)_6$	1 M $Zn(OAc)_2$ /[Ch]OAc	0.1	50 / -	[94]
Ionic liquid electrolyte	Zn	Pt/C	0.01 M ZnTfO/ DEMATfO	0.05	140 / 700	[95]
Ionic liquid electrolyte	Zn	-/C	1 M $Zn(OAc)_2$/[Ch]OAc	0.5 (A/g)	1000 / -	[96]

Ionic liquid electrolyte	Zn	-/C	0.2 M $Zn(TfO)_2$/ EMImTfO	0.2	100 / -	[97]
Solid-state electrolyte	Zn	Co/N-C	CH_2=CHCOOH/ $C_7H_{10}N_2O_2$ /11.25 M KOH /0.25 M ZnO /0.33 M $K_2S_2O_4$	10	125 / ~41	[98]
Solid-state electrolyte	Zn	Co/N-C/CoN_x/C	CH_2=CHCOOH/ $C_7H_{10}N_2O_2$ /11.25 M KOH/0.25 M ZnO /0.33 M $K_2S_2O_4$	1	68 / 25	[99]
Solid-state electrolyte	Zn	Co_3O_4 /C	6 M KOH /PVA/PEG/SiO_2	3	144 / 48	[100]
Solid-state electrolyte	Zn	Pt/C/Co_3O_4/C	KI/VAA/GO/KOH	2	200 / 200	[101]

* "-" : material is not provided. † "-" : measurement data is not available. ‡ "-" : measurement data is not available. § : mA (surface area is not reported). ‖ : coulomb. ¶ : mA g^{-1}.

Zhao et al.(2018) reported an integrated air electrode structure wherein the GDL and catalyst layers were combined.[5] Directly grown FeNi/N-CNT nanowire arrays on carbon cloth (CC) were attached on PTFE to produce an air cathode for a Zn-air battery (**Figure 3a and 3b**). Direct growth of FeNi/N-CNT on CC is desirable to enhance the electron transfer in the air cathode. Zn-air battery with a free-standing FeNi/N-CNT/CC air cathode produced stable charge (1.65 V) and discharge (1.0 V) voltages at a current density of 2 mA cm^{-2} for about 200 cycles (~33 hours testing time) of the charge-discharge test. Successful implementation of the direct-growth approach was also demonstrated in our previous work, where we utilized directly grown MnO_x on graphene-coated CC as the air cathode.[86] We achieved an all-solid-state, foldable, and rechargeable Zn-air battery with stable performance up to 175 cycles (~66 hours testing time).

Wang et al.(2019) reported a Zn-air battery with long cycle stability (~360 cycles, 240 hours testing time) using a composite of FeCo/FeCoNi/N-CNT hybrid fibers as a bifunctional electrocatalyst.[6] The cycling performance could be further enhanced for up to 1005 cycles (~670 hours testing time, **Figure 3c**) by utilizing FeCo/FeCoNi/N-CNT as the self-supported air cathode (i.e., FeCo/FeCoNi/N-CNT catalyst deposited on FeCo/FeCoNi/N-CNT membrane). The remarkable stability was attributed to the robust FeCo/FeCoNi/N-CNT structure and the stitched morphology of FeCo/FeCoNi alloy nanoparticles on the CNT support, which enhanced the oxygen adsorption and electron transfer.

Meanwhile, a more sustainable source of the catalyst has attracted significant attention to reduce the fabrication cost of Zn-air batteries further.[102] Marsudi et al.(2020) used table sugar-derived carbon decorated with MnO_2 nanorods as a bifunctional electrocatalyst in Zn-air batteries.[91] The carbon was obtained via facile dehydration of table sugar, and the MnO_2 nanorods were subsequently precipitated on the carbon surface using $KMnO_4$ as the precursor. The battery exhibited stable cycling stability for more than 215 cycles (~70 hours testing time). The use of an abundant and inexpensive material as the catalyst precursor such as biomass is one of the emerging research areas for the development of bifunctional electrocatalyst.

4.3. Electrolyte

The electrochemical behavior of secondary Zn–air batteries is highly influenced by the type of the electrolyte. Changes in electrolyte concentration, carbonate formation, and electrolyte leakage are some of the issues in Zn-air batteries that are related to the electrolyte. Moreover, several phenomena at the anode, such as corrosion and passivation, are also related to the type of electrolyte in Zn-air batteries.[92, 93, 103] Strategies to address the above problems include the addition of electrolyte additives, utilization of ionic liquids (ILs), and solid/semi-solid electrolytes.[41, 44, 104]

Mainar et al.(2018) added ZnO, KF, and K_2CO_3 to aqueous KOH solution as the electrolyte additives.[92] The incorporation of the additives accompanied by Nafion ionomer coating on the Zn anode had effectively suppressed the shape change, dendrite formation, and the HER rate. The Zn-air battery was stable during the prolonged charge-discharge test (10 cycles/~300 hours testing time). Kumar et al.(2019) then successfully prepared a Zn-air battery using water-soluble graphene (WSG) as an additive, which served as the corrosion inhibitor in 1 M KOH.[93] The water-soluble graphene suppressed the Zn corrosion rate. It also minimized gradual erosion of Zn during the self-discharge, which was attributed to the nano-coating of WSG on the Zn anode. However, it should be considered that the utilization of some additives may also cause negative effects, such as blocking the oxygen transfer in the air cathode.[105]

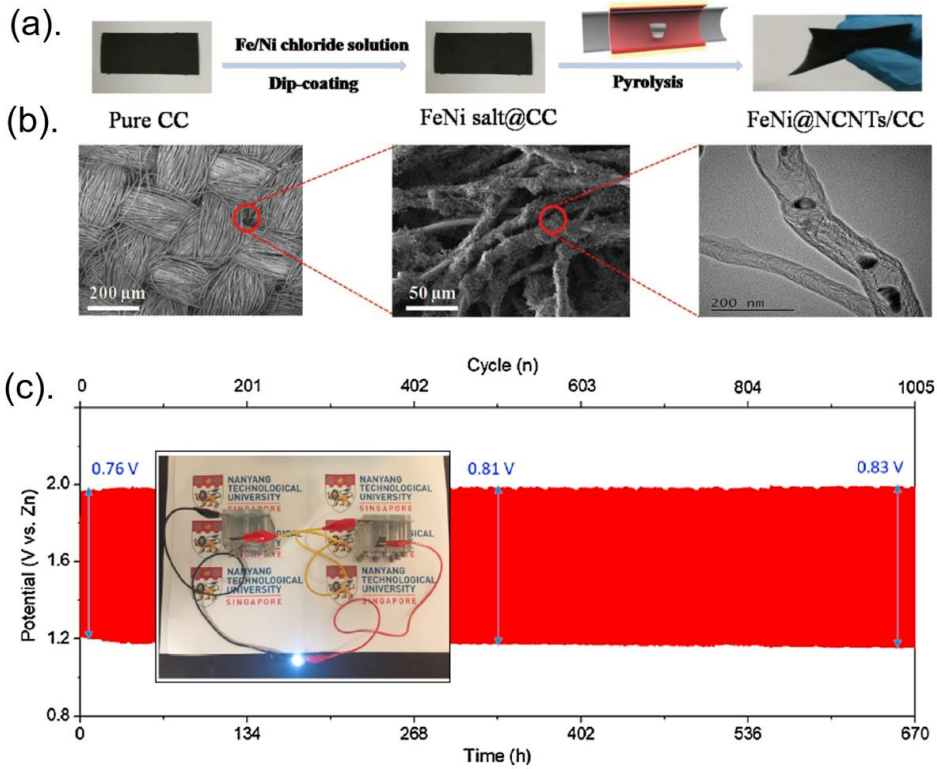

Figure 3. a) Schematic of the synthesis procedure for FeNi@NCNTs/CC. b) SEM (left and centre) and TEM (right) images of FeNi@NCNTs/CC. c) Charge-discharge stability test of Zn-air battery with self-supported FeCo/FeCoNi@NCNTs-HF air cathode at a current density of 5 mA cm^{-2} (Inset: images of the battery). (Adapted from ref. [5, 6] with copyright permission from John Wiley and Sons and Elsevier, respectively)

Ionic liquids (ILs) are another promising class of electrolytes for Zn-air batteries due to their non-volatility, non-flammability, high ionic conductivity, good chemical stability, and large density of charged ions.[106] Good room temperature ionic liquids (RTILs) are expected to enhance the cycle-life of the Zn-air battery by preventing passivation, self-discharge, water evaporation, and dendrite formation. In 2017, Ingale et al. utilized diethylmethylammonium trifluoromethanesulfonate (DEMATfO) as an ILs electrolyte in a secondary Zn-air battery.[95] The battery maintained a stable cell voltage for 140 cycles (~700 hours testing time) due to the improved reversibility of the Zn anode and reduced amounts of dendrite and carbonate formation. However, the high cost, as well as the low surface tension of DEMATfO, which potentially hinders the triple-phase reaction between the catalyst, oxygen, and ILs, pose challenges for their practical usage.

Zn-air batteries with aqueous-based electrolytes may leak due to the high internal pressure generated by the accumulation of gas in the air cathode. Hence, electrolyte modification in the form of solid or semi-solid electrolytes is pursued.[107, 108] Gel polymer electrolytes (GPEs) provide high ionic conductivity, mechanical stability, as well as corrosion and dendrite prevention. Fan et al.(2019) synthesized porous PVA nanocomposite as a host for alkaline-based GPE.[100] The schematic of the porous PVA-based nanocomposite GPE and its preparation method is shown in **Figure 4a**. The porous PVA-based alkaline GPE with the addition of 5 wt% SiO_2 exhibited satisfactory cycle-life of 144 cycles (~48 hours testing time), which was attributed to the high ionic conductivity and electrolyte retention capability of the GPEs. In addition, the charge-discharge test of the Zn-air battery under different bending conditions also showed excellent stability (**Figure 4b**). Recently, Song et al.(2020) demonstrated a long cycle-life Zn-air battery using semi-solid GPEs prepared by multiple crosslinking reactions among poly(vinyl alcohol), poly(acrylic acid), and KI modified GO.[101] The Zn-air battery using KI-PVAA-GO-KOH electrolyte exhibited a stable performance of up to 200 cycles (~200 hours testing time, **Figure 4c**). More importantly, the use of these GPEs improved the handleability of the Zn-air battery significantly, such that it could be suitable to power wearable devices, such as a commercial smartwatch (**Figure 4d**).

5. Battery configuration to enhance the cycle-life of Zn-air batteries

In addition to materials, battery configuration plays a major role in improving the cycle-life of secondary Zn-air batteries by mitigating the undesirable changes in the materials. Modifying the cell configuration can optimize the electrode performance and/or prevent the accumulation of zincate ions, which are beneficial to improve the cycle-life of Zn-air batteries.[1, 4] This section will discuss the advances in cell configuration such as the tri-electrode and flowing electrolyte configuration, which are promising approaches in improving the stability and cycle-life of Zn-air batteries.[1, 3, 109-111]

5.1. Tri-electrode configuration

Zn-air battery with the tri-electrode configuration was reportedly developed for the U.S. Army Electronic Command in 1988.[112] The tri-electrode configuration has the potential to enhance the

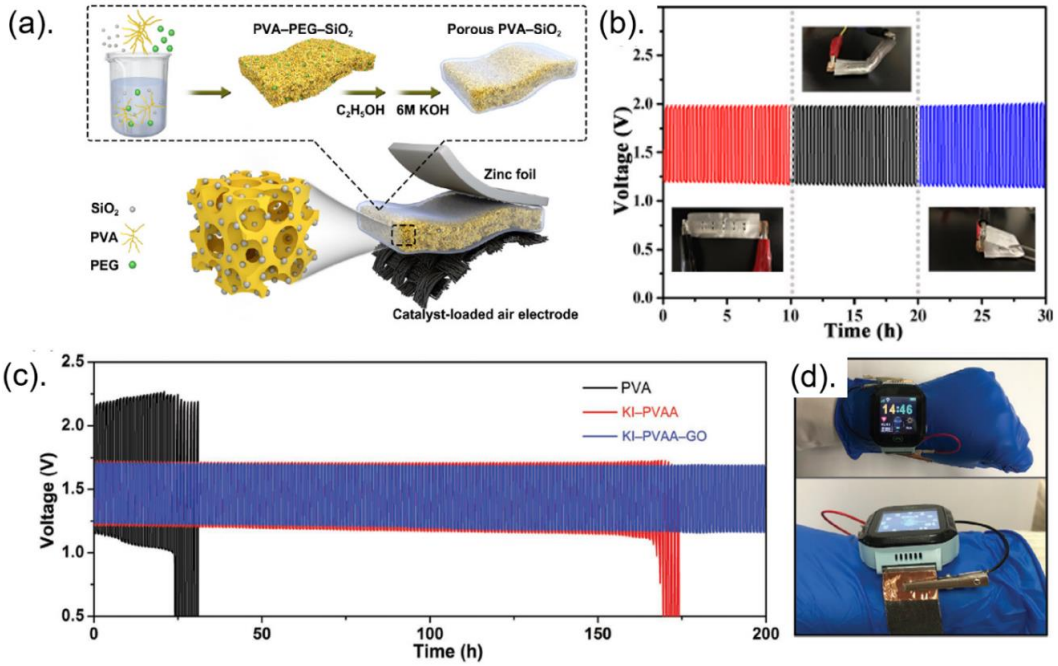

Fgure 4. a) Schematic synthesis of the porous PVA-based nanocomposite GPE. b) Charge-discharge curves of Zn-air battery under different bending conditions. c) Charge-discharge curves of Zn-air battery using PVA, PVAA–GO, and KI–PVAA–GO GPEs at 2 mA cm-2. d) Photographs of three units of Zn-air batteries to power a commercial smartwatch. (Adapted from ref. [89, 90] with copyright permission from Elsevier and John Wiley and Sons, respectively)

cycle-life of the conventional bi-electrode Zn-air battery as the charge and discharge processes are performed by different air cathodes (i.e., ORR electrode and OER electrode), where the Zn anode is usually vertically positioned between the two electrodes. With this configuration, different OER and ORR catalysts can be deposited on the separate air cathode, such that the charge and discharge processes can be optimized accordingly. Despite the breakthrough design, we note that common issues such as shape change and corrosion at the electrodes can still occur, and improvement strategies elaborated in earlier sections can be applied to improve the performance further.

The use of aqueous electrolytes often leads to leakage during the prolonged operation of the Zn-air battery. Tran et al. (2020) employed poly(acrylic acid)-based GPEs in a Zn-air battery with a tri-electrode configuration to reduce the risk of electrolyte leakage.[4] The battery was fabricated by sandwiching the Zn electrode in between the ORR top electrode and the OER bottom electrode (**Figure 5c**). This configuration was able to mitigate the corrosion of Zn and accumulation of O_2 gas bubbles. The battery showed a relatively stable performance of up to 100 cycles (~50 hours testing time).

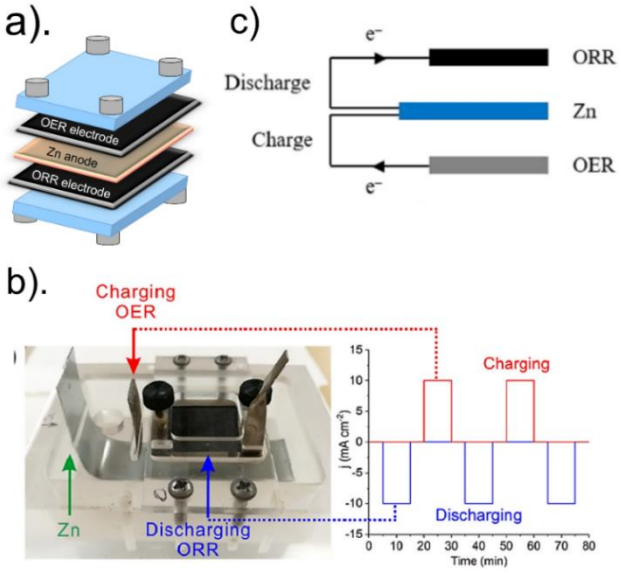

Figure 5. Configuration of a) horizontal tri-electrode, b) hybrid tri-electrode Zn-air battery (left) and the current waveform during the discharge-charge test (right), and c) tri-electrode Zn-air battery using GPEs sandwich. (Adapted from ref. [3, 4] with copyright permission from Elsevier)

Hong et al.(2016) developed a secondary Zn-air battery using a tri-electrode structure in a horizontal configuration.[109] The OER electrode, Zn anode, and ORR electrode were horizontally positioned at the top, middle, and bottom of the battery, respectively (**Figure 5a**). This strategy can effectively eliminate the gravity effect on the Zn anode that can reduce the dendrite growth and shape change of the Zn anode during the charge-discharge test. As a result, remarkable cycling performance for about 1000 cycles (~1917 hours testing time) was achieved during the measurement. Furthermore, this work enabled the generated oxygen to easily diffuse during charging, as well as preventing the loss of catalyst and physical/chemical degradation of the air cathode.

Xiong et al.(2018) improved the tri-electrode configuration further using the ORR and OER electrodes that are placed differently (**Figure 5b**).[3] The ORR electrode was placed horizontally on top of the cell to reduce the electrolyte pressure, while the OER electrode was positioned vertically to avoid O_2 buildup during the OER process. Using MnO_x and Co-Fe/Ni catalyst, this battery showed a stable performance of up to 120 cycles (~50 hours testing time). Other notable works on Zn-air batteries with tri-electrode configuration are summarized in **Table 3**.

5.2. Flowing electrolyte configuration

The flowing electrolyte configuration is another innovative approach borrowed from the redox flow batteries strategy that can be adopted to improve the cycle-life of the Zn-air battery.[113] Research interest in this area is rapidly growing, with flow Zn-air batteries consistently showing excellent durability.[1, 110, 114, 115] Although most of the main components are similar to conventional static Zn-air batteries, the electrolyte is continually circulated through an external reservoir and pump (**Figure 6a**). The flowing electrolyte introduces fresh electrolyte that can even out the ionic composition across the electrodes. This way, excessive concentration of zincate ions, along with any insoluble precipitates (possibly including some of the oxide deposits on the Zn anode and outgrowing Zn dendrites), can be swept out and filtered, effectively alleviating the negative impacts of these species on the cycle-life.[116] The external reservoir also allows for easy electrolyte replenishment or maintenance. The most recent development of Zn-air batteries that use the flowing electrolyte configuration is summarized in **Table 4**.

Bockelmann et al.(2016) prepared a Zn-air flow battery using aqueous KOH as the electrolyte.[114] A silver-containing oxygen depolarized air cathode with high catalytic activity and excellent long-term stability was incorporated into the battery. The battery showed a stable cycling performance for more than 600 cycles, without the need to replace the Zn anode and the electrolyte. Recently, Khezri et al.(2020) tried to enhance the cycling performance of rechargeable Zn-air flow batteries using the additives incorporated KOH-based electrolyte.[115] It was proven that potassium persulfate (KPS) at a low concentration (450 ppm) could enhance the kinetics of the oxidation reaction by accelerating Zn oxidation and zincate formation. In particular, the battery using such an additive exhibited long cycle-life of more than 800 cycles.

To further optimize the flowing electrolyte configuration, Yu et al.(2020) investigated the effect of flow rate and flow orientation on the Zn electrode.[1] It was suggested that the life span of the battery using the Zn anode could be enhanced by increasing the electrolyte

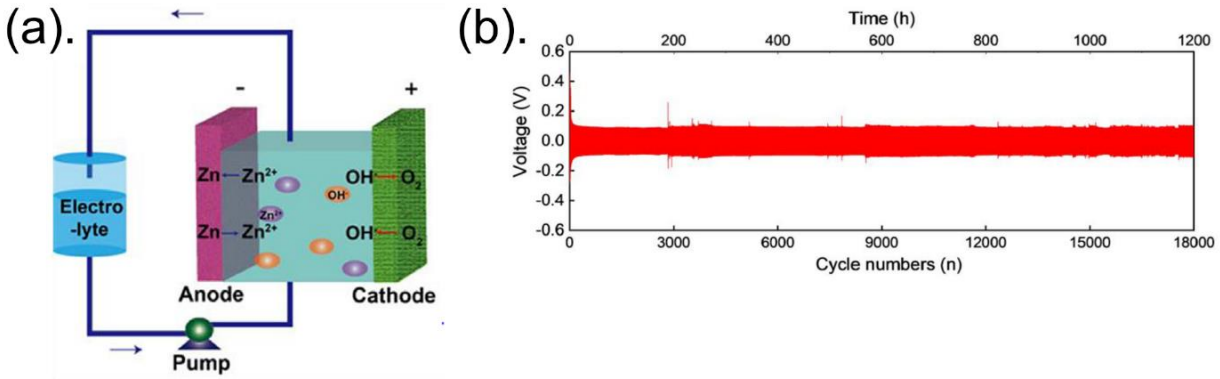

Figure 6. a) Schematic of secondary Zn-air flow battery. b) Cycle-life of the battery using a direct flow channel. (Adapted from ref. [1, 2] with copyright permission from Elsevier)

flow rate. Using 50 rad min^{-1} of the flow rate, the battery cycle-life can be enhanced to 4725 cycles, five times longer than the 10 rad min^{-1} flow rate. The high rate of electrolyte flow effectively balanced the deposited zinc rate on the anode surface and suppressed the dendrite growth on the anode. Moreover, the evenly distributed concentration of zincate ions improved the stability and cycle-life of the battery. Using this strategy, the cycle-life of the battery was enhanced up to 18000 cycles (~1200 hours testing time) (**Figure 6b**).

Table 3. Cycling stability of aqueous Zn-air batteries using the tri-electrode configuration in literature

ORR electrode	OER electrode	Counter electrode	Electrolyte	Current density (mA cm^{-2})	Cycling stability (cycle/hour)	Ref.
CoO/N-C/C	NiFe/Ni	Zn	6 M KOH/ 0.2 M $Zn(OAc)_2$	20	10 / 200	[117]
CoPS/C	CoPS/C	Zn	6 M KOH/ 0.2 M $Zn(OAc)_2$	20	100 / 100	[118]
Mn/MnO/PTFE/C/Ni	RuO_2	Zn	6 M KOH /0.4 M ZnO	20	1000 / 1917	[109]
MnO_x/C	CoFe/Ni	Zn	6 M KOH/0.25 M ZnO	10	120 / 50	[3]
MnO_x/C	CoFe/Ni	Zn	7.5 M KOH/ 0.25 M ZnO/PAA	5	100 / 50	[4]
Mn_3O_4/C	Ni	Zn	6 M KOH/0.25 ZnO	20	235 / 117.5	[119]
N,P-C	N,P-C	Zn	6 M KOH	2	600 / 100	[82]
P,S-C	P,S/C	Zn	7.5 M KOH /0.25 M ZnO	25	500 / 100	[120]

Table 4. Cycling stability of secondary Zn-air batteries using flowing electrolyte configuration in literature

Catalyst/gas diffusion electrode	Anode	Electrolyte	Current density during cycling test (mA cm^{-2})	Cycling stability (cycle/hour)*	Ref.
Ag/Ni	Zn	KOH/ZnO	50	600 / -	[114]
FeNi/SiO_2/COP	Zn	8 M KOH/0.5 ZnO	10	45 / 90	[121]
FeP/Fe_2O_3/N,P/C	Zn	KOH/$Zn(OAc)_2$	5	1590 / 265	[122]
IrO_2/C	Zn	8 M KOH/0.5 ZnO/COF_{BTC}	10	40 / 80	[123]
MnO_2/Ni/PTVE/C	Zn	7 M KOH/0.5 M ZnO/KPS	5†	800 / -	[115]
Pt/C/PVA/IrO_2/C	Zn	8 M KOH/0.5 M ZnO	10	50 / 100	[2]

* **"-" :** measurement data is not available. † : mA h

6. Summary and outlook

Despite the formidable technical challenges described above, Zn-air batteries are still one of the most promising secondary battery systems: they are affordable, inherently safe, and environmentally friendly with high theoretical energy density. With concerted and targeted research, careful observation and failure analysis are the first steps in uncovering the dominant failure mechanisms that cause the short cycle-life in Zn-air batteries. More importantly, the underlying materials and engineering issues must be correctly identified to guide effective materials engineering and cell architecture redesign to improve the performance of Zn-air batteries.

Modification of the Zn anode is typically done by combining or coating the anode with other elements, such as heavy metals, carbon, or organic materials. These modifications are primarily aimed at suppressing one or several of the following phenomena: (1) HER, (2) shape change, (3) corrosion, (4) deposition of a passivation layer, and (5) dendrite growth. At the air cathode, the modification can be focused on the GDLs. New classes of GDLs with better corrosion resistance and pore structure are continually being proposed to replace conventional nickel foam and carbon paper based GDLs. Another modification on the air cathode is aimed at finding more

robust and efficient bifunctional O_2 electrocatalysts. This is a tough challenge, as the suitable electrocatalyst would need to be extremely active and stable in both cathodic (ORR) and anodic (OER) conditions, with as small onset electrochemical window as possible. Typically, alloying or heterostructuring is required to optimize the binding energy of the reaction intermediates and increase the conductivity at the same time. The catalyst surface area also needs to be increased to expose a larger number of active sites. Besides that, the development of new electrocatalysts must also consider the cost-effectiveness and sustainability aspects. On the electrolyte part, incorporation of the additives and ILs is the low hanging fruit, as it results in a much more stable cycling performance with traditional liquid electrolyte architecture. We predict that solid and semi-solid electrolytes will play an important role in new generations of Zn-air batteries, as modern wearable electronics and aerial vehicles demand multi-functioning structural batteries with improved mechanical strength, shape flexibility, safety, and long-term service life.

Radical design changes, such as the tri-electrode configuration and the flowing electrolyte configuration, are some out-of-the-box solutions developed by correctly identifying the underlying engineering issues of Zn-air battery architectures. These configurations can effectively hinder the mechanical loss of the catalyst and corrosion of the air cathode. In particular, the tri electrode configuration not only alleviates the gas accumulation on the Zn anode, but also enhances the air cathode performance since the ORR and OER processes can now be performed by specialized catalysts on physically separated air electrodes. The flowing electrolyte configuration borrows the concept from redox flow batteries. It can effectively improve the durability of Zn-air batteries by alleviating the adverse effects associated with the reaction by-products as the fresh electrolyte is continually being circulated throughout the battery through an external reservoir.

Beyond improving the stability and cycle-life performance, widespread adoption of secondary Zn-air batteries requires research and development tailored to the target applications. At present, we identified several large markets suitable for Zn-air battery penetration: (1) grid energy storage, (2) automotive and aerospace sectors, and (3) miniaturized devices. The grid storage application would require research and development that focuses on increasing power and energy density that could benefit from the flow electrolyte configuration. Further improvement of flow electrolyte configuration can be achieved by optimizing electrolyte composition, viscosity, and flow path architecture. The automotive and aerospace systems require reliable batteries that can deliver high current bursts, with paramount emphasis on safety and fail-safe design. This can be achieved by combining the tri-electrode configuration with the proven valve-regulated system in the traditional lead-acid that prevents gas accumulation. Solid and semi-solid electrolytes may also be particularly attractive to aerospace applications as they limit the risk of leakage and offer ease of handling. Powering miniaturized and wearable devices can be achieved by focusing on delivering a compact and flexible design, of which semi-solid or solid electrolyte and improved GDLs architecture will also play a significant role.

Conflicts of interest

There are no conflicts to declare.

Acknowledgements

A.D.H. acknowledges funding support from the Agency for Science, Technology and Research (A19E9a0103 and A20B3a0133). A.S. acknowledges the funding from the Indonesian Ministry of Research, Technology and Higher Education under the WCU Program managed by Institut Teknologi Bandung. A.S. also thanks the support from the Indonesia Endowment Fund for Education (LPDP).

Keywords: Metal-air battery •Zinc battery• secondary battery• cycling stability• electrocatalyst

[1] W. Yu, W. Shang, X. Xiao, P. Tan, B. Chen, Z. Wu, H. Xu, M. Ni, *J. Power Sources* **2020**, 453, 227856.
[2] N. Zhang, C. Deng, S. Tao, L. Guo, Y. Cheng, *Chem. Eng. Sci.* **2020**, 224, 115795.
[3] M. Xiong, M. P. Clark, M. Labbe, D. G. Ivey, *J. Power Sources* **2018**, 393, 108-118.
[4] T. N. T. Tran, M. P. Clark, M. Xiong, H.-J. Chung, D. G. Ivey, *Electrochim. Acta* **2020**, 357, 136865.
[5] X. Zhao, S. C. Abbas, Y. Huang, J. Lv, M. Wu, Y. Wang, *Adv. Mater. Interfaces* **2018**, 5, 1701448.
[6] Z. Wang, J. Ang, B. Zhang, Y. Zhang, X. Y. D. Ma, T. Yan, J. Liu, B. Che, Y. Huang, X. Lu, *Appl. Catal., B* **2019**, 254, 26-36.
[7] Y.-S. Lee, Y.-J. Kim, K.-S. Ryu, *J. Ind. Eng. Chem.* **2019**, 78, 295-302.
[8] Y. Zhang, Y. Wu, W. You, M. Tian, P. W. Huang, Y. Zhang, Z. Sun, Y. Ma, T. Hao, N. Liu, *Nano Lett.* **2020**.
[9] J. Hao, X. Li, S. Zhang, F. Yang, X. Zeng, S. Zhang, G. Bo, C. Wang, Z. Guo, *Adv. Funct. Mater.* **2020**, 2001263.
[10] A. Hagfeldt, G. Boschloo, L. Sun, L. Kloo, H. Pettersson, *Chem. Rev.* **2010**, 110, 6595-6663.
[11] C. Liu, F. Li, L. P. Ma, H. M. Cheng, *Adv. Mater.* **2010**, 22, E28-E62.
[12] Z.-L. Wang, D. Xu, H.-X. Zhong, J. Wang, F.-L. Meng, X.-B. Zhang, *Sci. Adv.* **2015**, 1, e1400035.
[13] M. Iizuka, *Innovation and Development* **2015**, 5, 241-261.
[14] J. M. Carrasco, L. G. Franquelo, J. T. Bialasiewicz, E. Galván, R. C. PortilloGuisado, M. M. Prats, J. I. León, N. Moreno-Alfonso, *IEEE Trans. Ind. Electron.* **2006**, 53, 1002-1016.
[15] M. M. MR Weimar, T Levin, A Botterud, E O'Shaughnessy, L Bird, *Integrating Renewable Generation into Grid Operations*, **2016**.
[16] S. Tselepis, J. Nikoletatos, *IEA-Etsap Irena Technology Brief* **2015**.
[17] N. E. T. Laboratory, *Energy Storage–A Key Enabler of The Smart Grid*, **2009**.
[18] K. K. Zame, C. A. Brehm, A. T. Nitica, C. L. Richard, G. D. Schweitzer III, *Renewable Sustainable Energy Rev.* **2018**, 82, 1646-1654.
[19] J. Fu, Z. P. Cano, M. G. Park, A. Yu, M. Fowler, Z. Chen, *Adv. Mater.* **2017**, 29, 1604685.
[20] M. Li, J. Lu, Z. Chen, K. Amine, *Adv. Mater.* **2018**, 30, 1800561.
[21] M. Winter, B. Barnett, K. Xu, *Chem. Rev.* **2018**, 118, 11433-11456.
[22] N. Nitta, F. Wu, J. T. Lee, G. Yushin, *Mater. Today* **2015**, 18, 252-264.

[23] J. B. Goodenough, K.-S. Park, *J. Am. Chem. Soc.* **2013**, 135, 1167-1176.
[24] A. K. Thapa, T. Ishihara, *J. Power Sources* **2011**, 196, 7016-7020.
[25] B. T. Hang, M. Eashira, I. Watanabe, S. Okada, J.-I. Yamaki, S.-H. Yoon, I. Mochida, *J. Power Sources* **2005**, 143, 256-264.
[26] Z. Chen, A. Yu, D. Higgins, H. Li, H. Wang, Z. Chen, *Nano letters* **2012**, 12, 1946-1952.
[27] A. Kraytsberg, Y. Ein-Eli, *J. Power Sources* **2011**, 196, 886-893.
[28] L. Li, Z. w. Chang, X. B. Zhang, *Adv. Sustainable Syst.* **2017**, 1, 1700036.
[29] H.-G. Jung, J. Hassoun, J.-B. Park, Y.-K. Sun, B. Scrosati, *Nat. Chem.* **2012**, 4, 579.
[30] G. Girishkumar, B. McCloskey, A. C. Luntz, S. Swanson, W. Wilcke, *J. Phys. Chem. Lett.* **2010**, 1, 2193-2203.
[31] H. Vikström, S. Davidsson, M. Höök, *Appl. Energy* **2013**, 110, 252-266.
[32] A. Smee, *The London, Edinburgh, and Dublin Philosophical Magazine and Journal of Science* **1840**, 16, 315-321.
[33] B. Beverskog, I. Puigdomenech, *Corros. Sci.* **1997**, 39, 107-114.
[34] J. Goldstein, I. Brown, B. Koretz, *J. Power Sources* **1999**, 80, 171-179.
[35] T. B. Reddy, *Linden's handbook of batteries*, Mcgraw-hill New York **2011**.
[36] X. F. Lu, Y. Chen, S. Wang, S. Gao, X. W. Lou, *Adv. Mater.* **2019**, 31, 1902339.
[37] G. Fu, Y. Tang, J. M. Lee, *ChemElectroChem* **2018**, 5, 1424-1434.
[38] U. G. Survey, *Journal* **2020**.
[39] Y. Nam Jo, P. Santhoshkumar, K. Prasanna, K. Vediappan, C. Woo Lee, *J. Ind. Eng. Chem.* **2019**, 76, 396-402.
[40] P. Pei, K. Wang, Z. Ma, *Appl. Energy* **2014**, 128, 315-324.
[41] M. Xu, D. Ivey, Z. Xie, W. Qu, *J. Power Sources* **2015**, 283, 358-371.
[42] J. Pan, Y. Y. Xu, H. Yang, Z. Dong, H. Liu, B. Y. Xia, *Adv. Sci.* **2018**, 5, 1700691.
[43] A. R. Mainar, E. Iruin, L. C. Colmenares, A. Kvasha, I. de Meatza, M. Bengoechea, O. Leonet, I. Boyano, Z. Zhang, J. A. Blazquez, *J. Storage Mater.* **2018**, 15, 304-328.
[44] X. Chen, Z. Zhou, H. E. Karahan, Q. Shao, L. Wei, Y. Chen, *Small* **2018**, 14, 1801929.
[45] J. Zhang, Q. Zhou, Y. Tang, L. Zhang, Y. Li, *Chem. Sci.* **2019**, 10, 8924-8929.
[46] K. J. Lopez, J.-H. Yang, H.-J. Sun, G. Park, S. Eom, H.-R. Rim, H.-K. Lee, J. Shim, *Transactions of the Korean hydrogen and new energy society* **2016**, 27, 677-684.
[47] E. L. Dewi, K. Oyaizu, H. Nishide, E. Tsuchida, *J. Power Sources* **2003**, 115, 149-152.
[48] J. Shin, J. Lee, Y. Park, J. W. Choi, *Chem. Sci.* **2020**, 11, 2028-2044.
[49] X. Ge, A. Sumboja, D. Wuu, T. An, B. Li, F. T. Goh, T. A. Hor, Y. Zong, Z. Liu, *ACS Catal.* **2015**, 5, 4643-4667.
[50] B. Hwang, E.-S. Oh, K. Kim, *Electrochim. Acta* **2016**, 216, 484-489.
[51] A. Sumboja, X. Ge, G. Zheng, F. T. Goh, T. A. Hor, Y. Zong, Z. Liu, *J. Power Sources* **2016**, 332, 330-336.
[52] Y. Wu, Y. Zhang, Y. Ma, J. D. Howe, H. Yang, P. Chen, S. Aluri, N. Liu, *Adv. Energy Mater.* **2018**, 8, 1802470.
[53] V. Caldeira, R. Rouget, F. Fourgeot, J. Thiel, F. Lacoste, L. Dubau, M. Chatenet, *J. Power Sources* **2017**, 350, 109-116.
[54] W. Gan, D. Zhou, J. Zhao, L. Zhou, *J. Appl. Electrochem.* **2015**, 45, 913-919.
[55] F. Santos, J. Abad, M. Vila, G. R. Castro, A. Urbina, A. J. Fernández Romero, *Electrochim. Acta* **2018**, 281, 133-141.
[56] S.-M. Lee, Y.-J. Kim, S.-W. Eom, N.-S. Choi, K.-W. Kim, S.-B. Cho, *J. Power Sources* **2013**, 227, 177-184.
[57] L. Li, A. Manthiram, *Adv. Energy Mater.* **2016**, 6, 1502054.
[58] M. J. Tan, B. Li, P. Chee, X. Ge, Z. Liu, Y. Zong, X. J. Loh, *J. Power Sources* **2018**, 400, 566-571.
[59] M. S. Naughton, F. R. Brushett, P. J. Kenis, *J. Power Sources* **2011**, 196, 1762-1768.
[60] C. Shenghai, S. Liping, K. Fanhao, H. Lihua, Z. Hui, *J. Power Sources* **2019**, 430, 25-31.
[61] D. Lu, J. Li, J. He, R. Zhao, Y. Cai, *J. Phys. Chem. C* **2019**, 123, 8522-8530.
[62] S. Lysgaard, M. K. Christensen, H. A. Hansen, J. M. García Lastra, P. Norby, T. Vegge, *ChemSusChem* **2018**, 11, 1933-1941.
[63] Y. Sun, X. Liu, Y. Jiang, J. Li, J. Ding, W. Hu, C. Zhong, *J. Mater. Chem. A* **2019**, 7, 18183-18208.
[64] R. Othman, A. Yahaya, A. Arof, *J. Appl. Electrochem.* **2002**, 32, 1347-1353.
[65] M. N. Masri, A. A. Mohamad, *J. Electrochem. Soc.* **2013**, 160, A715.
[66] D. Ozgit, P. Hiralal, G. A. Amaratunga, *ACS Appl. Mater. Interfaces* **2014**, 6, 20752-20757.
[67] S.-H. Lee, D.-J. Park, W.-G. Yang, K.-S. Ryu, *Ionics* **2017**, 23, 1801-1809.
[68] Z. Zhou, Y. Zhang, P. Chen, Y. Wu, H. Yang, H. Ding, Y. Zhang, Z. Wang, X. Du, N. Liu, *Chem. Eng. Sci.* **2019**, 194, 142-147.
[69] H. S. Kim, Y. N. Jo, W. J. Lee, K. J. Kim, C. W. Lee, *Electroanalysis* **2015**, 27, 517-523.
[70] Z. Zhang, D. Zhou, X. Bao, L. Zhou, J. Zhao, B. Huang, *J. Solid State Electrochem.* **2018**, 22, 3775-3783.
[71] A. Xia, X. Pu, Y. Tao, H. Liu, Y. Wang, *Appl. Surf. Sci.* **2019**, 481, 852-859.
[72] Z. Ma, P. Pei, K. Wang, X. Wang, H. Xu, Y. Liu, *J. Power Sources* **2015**, 274, 56-64.
[73] D. U. Lee, J. Y. Choi, K. Feng, H. W. Park, Z. Chen, *Adv. Energy Mater.* **2014**, 4, 1301389.
[74] P. Moni, A. Deschamps, D. Schumacher, K. Rezwan, M. Wilhelm, *J. Colloid Interface Sci.* **2020**, 577, 494-502.
[75] D. Lee, H. Lee, O. Gwon, O. Kwon, H. Y. Jeong, G. Kim, S.-Y. Lee, *J. Mater. Chem. A* **2019**, 7, 24231-24238.
[76] J. Mei, T. Liao, J. Liang, Y. Qiao, S. X. Dou, Z. Sun, *Adv. Energy Mater.* **2020**, 10, 1901997.
[77] Q. Liu, Z. Pan, E. Wang, L. An, G. Sun, *Energy Storage Mater.* **2020**, 27, 478-505.
[78] X. Yu, T. Zhou, J. Ge, C. Wu, *ACS Mater. Lett.* **2020**, 2, 1423-1434.
[79] C. W. Lee, K. Sathiyanarayanan, S. W. Eom, M. S. Yun, *J. Power Sources* **2006**, 160, 1436-1441.
[80] Y.-D. Cho, G. T.-K. Fey, *J. Power Sources* **2008**, 184, 610-616.
[81] J. Huang, Z. Yang, R. Wang, Z. Zhang, Z. Feng, X. Xie, *J. Mater. Chem. A* **2015**, 3, 7429-7436.
[82] J. Zhang, Z. Zhao, Z. Xia, L. Dai, *Nat. Nanotechnol.* **2015**, 10, 444-452.
[83] A. Sumboja, X. Ge, F. T. Goh, B. Li, D. Geng, T. A. Hor, Y. Zong, Z. Liu, *ChemPlusChem* **2015**, 80, 1341.
[84] M. Lubke, A. Sumboja, L. McCafferty, C. F. Armer, A. D. Handoko, Y. Du, K. McColl, F. Cora, D. Brett, Z. Liu, *ChemistrySelect* **2018**, 3, 2613-2622.
[85] A. Sumboja, J. Chen, Y. Zong, P. S. Lee, Z. Liu, *Nanoscale* **2017**, 9, 774-780.
[86] A. Sumboja, M. Lübke, Y. Wang, T. An, Y. Zong, Z. Liu, *Adv. Energy Mater.* **2017**, 7, 1700927.
[87] T. An, X. Ge, N. N. Tham, A. Sumboja, Z. Liu, Y. Zong, *ACS Sustainable Chem. Eng.* **2018**, 6, 7743-7751.
[88] M. Wu, B. Guo, A. Nie, R. Liu, *J. Colloid Interface Sci.* **2020**, 561, 585-592.
[89] X. Zheng, X. Cao, Z. Sun, K. Zeng, J. Yan, P. Strasser, X. Chen, S. Sun, R. Yang, *Appl. Catal., B* **2020**, 272, 118967.
[90] Y. Xu, A. Sumboja, Y. Zong, J. A. Darr, *Catal. Sci. Technol.* **2020**, 10, 2173-2182.
[91] M. A. Marsudi, Y. Ma, B. Prakoso, J. J. Hutani, A. Wibowo, Y. Zong, Z. Liu, A. Sumboja, *Catalysts* **2020**, 10, 64.
[92] A. R. Mainar, L. C. Colmenares, H.-J. Grande, J. A. Blázquez, *Batteries* **2018**, 4, 46.
[93] K. K. Kumar, R. Brindha, M. Nandhini, M. Selvam, K. Saminathan, K. Sakthipandi, *Ionics* **2019**, 25, 1699-1706.
[94] Z. Liu, P. Bertram, F. Endres, *J. Solid State Electrochem.* **2017**, 21, 2021-2027.
[95] P. Ingale, M. Sakthivel, J. F. Drillet, *J. Electrochem. Soc.* **2017**, 164, H5224-H5229.
[96] Z. Liu, G. Li, T. Cui, A. Borodin, C. Kuhl, F. Endres, *J. Solid State Electrochem.* **2018**, 22, 91-101.

[97] J. Fan, Q. Xiao, Y. Fang, L. Li, W. Yuan, *Ionics* **2019**, 25, 1303-1313.
[98] W. Zang, A. Sumboja, Y. Ma, H. Zhang, Y. Wu, S. Wu, H. Wu, Z. Liu, C. Guan, J. Wang, S. J. Pennycook, *ACS Catal.* **2018**, 8, 8961-8969.
[99] C. Guan, A. Sumboja, W. Zang, Y. Qian, H. Zhang, X. Liu, Z. Liu, D. Zhao, S. J. Pennycook, J. Wang, *Energy Storage Mater.* **2019**, 16, 243-250.
[100] X. Fan, J. Liu, Z. Song, X. Han, Y. Deng, C. Zhong, W. Hu, *Nano Energy* **2019**, 56, 454-462.
[101] Z. Song, J. Ding, B. Liu, X. Liu, X. Han, Y. Deng, W. Hu, C. Zhong, *Adv. Mater.* **2020**, 32, 1908127.
[102] C. Zhao, G. Liu, N. Sun, X. Zhang, G. Wang, Y. Zhang, H. Zhang, H. Zhao, *Chem. Eng. J.* **2018**, 334, 1270-1280.
[103] M. C. Huang, S. H. Huang, S. C. Chiu, K. L. Hsueh, W. S. Chang, C. C. Yang, C. C. Wu, J. C. Lin, *J. Chin. Chem. Soc.* **2018**, 65, 1239-1244.
[104] A. Sumboja, P. L. Sambegoro, A Stability Improvement of Rechargeable Zn-air Batteries by Introducing Thiourea and Polyethylenimine as Electrolyte Additives, Surakarta, Indonesia, 2018.
[105] P. Chen, K. Zhang, D. Tang, W. Liu, F. Meng, Q. Huang, J. Liu, *Front. Chem.* **2020**, 8.
[106] H. Ohno, M. Yoshizawa, W. Ogihara, *Electrochim. Acta* **2004**, 50, 255-261.
[107] A. Sumboja, J. Chen, Y. Ma, Y. Xu, Y. Zong, P. S. Lee, Z. Liu, *ChemCatChem* **2019**, 11, 1205-1213.
[108] C. Guan, A. Sumboja, H. Wu, W. Ren, X. Liu, H. Zhang, Z. Liu, C. Cheng, S. J. Pennycook, J. J. A. M. Wang, *Adv. Mater.* **2017**, 29, 1704117.
[109] W. Hong, H. Li, B. Wang, *Int. J. Electrochem. Sci.* **2016**, 11, 3843-3851.
[110] S. Hosseini, W. Lao-atiman, S. J. Han, A. Arpornwichanop, T. Yonezawa, S. Kheawhom, *Sci. Rep.* **2018**, 8, 14909.
[111] A. Abbasi, S. Hosseini, A. Somwangthanaroj, R. Cheacharoen, S. Olaru, S. Kheawhom, *Sci. Data* **2020**, 7, 196.
[112] R. Sen, S. Van Voorhees, T. Ferrel, *Metal-air battery assessment*, Pacific Northwest Lab., Richland, WA (USA), **1988**.
[113] T.-N. Pham-Truong, Q. Wang, J. Ghilane, H. Randriamahazaka, *ChemSusChem* **2020**, 13, 2142-2159.
[114] M. Bockelmann, U. Kunz, T. Turek, *Electrochem. Commun.* **2016**, 69, 24-27.
[115] R. Khezri, S. Hosseini, A. Lahiri, S. R. Motlagh, M. T. Nguyen, T. Yonezawa, S. Kheawhom, *Int. J. Mol. Sci.* **2020**, 21, 7303.
[116] R. Naybour, *J. Electrochem. Soc.* **1969**, 116, 520.
[117] Y. Li, M. Gong, Y. Liang, J. Feng, J.-E. Kim, H. Wang, G. Hong, B. Zhang, H. Dai, *Nat. Commun.* **2013**, 4, 1805.
[118] B. Roy, K. J. Shebin, S. Sampath, *J. Power Sources* **2020**, 450, 227661.
[119] Y. He, D. Aasen, H. Yu, M. Labbe, D. G. Ivey, J. G. C. Veinot, *Nanoscale Adv.* **2020**, 2, 3367-3374.
[120] S. S. Shinde, C.-H. Lee, A. Sami, D.-H. Kim, S.-U. Lee, J.-H. Lee, *ACS Nano* **2017**, 11, 347-357.
[121] J. Guo, T. Li, Q. Wang, N. Zhang, Y. Cheng, Z. Xiang, *Nanoscale* **2019**, 11, 211-218.
[122] K. Wu, L. Zhang, Y. Yuan, L. Zhong, Z. Chen, X. Chi, H. Lu, Z. Chen, R. Zou, T. Li, *Adv. Mater.* **2020**, 32, 2002292.
[123] P. Peng, L. Shi, F. Huo, S. Zhang, C. Mi, Y. Cheng, Z. Xiang, *ACS Nano* **2019**, 13, 878-884.